Faraday Discussions

Cite this: *Faraday Discuss.*, 2022, **237**, 381

ROYAL SOCIETY OF CHEMISTRY

PAPER

View Article Online
View Journal | View Issue

Modelling nonlocal nonlinear spin dynamics in antiferromagnetic orthoferrites†

Yuichi Saito and Rostislav V. Mikhaylovskiy *

Received 7th February 2022, Accepted 6th April 2022
DOI: 10.1039/d2fd00035k

Excitation with an ultrashort light pulse is arguably the only way to control spins in antiferromagnetic materials at both the nanoscale in space and ultrafast time scale. While recent experiments highlighted tantalising opportunities for spin switching and magnonics in antiferromagnets, the theoretical description of antiferromagnetic spin dynamics driven by strongly localised and ultrashort excitation is in its infancy. Here we report a theoretical model describing the nonlocal and nonlinear spin response to the excitation by light. We show that strongly localised ultrafast excitation can drive spin switching, which propagates in space and acts as a source of spin waves. Our theoretical formalism is readily available to describe current and future ultrafast spectroscopy experiments in antiferromagnets.

Introduction

Antiferromagnets, materials supporting magnetic ordering without net magnetization, are the most appealing media for future technologies in ultrafast and energy efficient data storage and computing, based on spintronics and magnonics.[1,2] In particular, antiferromagnets have the magnetic resonance frequency in the sub-terahertz or terahertz (THz) region and therefore produce a much faster coherent response to external perturbation, compared to the conventional ferromagnets, whose resonance frequencies lie in the gigahertz range. Also, strong magneto-optical coupling in many antiferromagnets ensures good susceptibility of their magnetic order to illumination with laser pulses.[3] Therefore, the advent of femtosecond lasers has opened the way to create external stimuli that are shorter than characteristic timescales such as spin-lattice relaxation or spin precession period, thereby enabling ultrafast manipulation of the antiferromagnetic states.[4] Moreover, the development of technology generating intense THz fields, especially the tilted pulse front method,[5] allows researchers to excite spin dynamics in antiferromagnets *via* direct resonant mechanisms.[6,7]

Department of Physics, Lancaster University, Bailrigg, Lancaster LA1 4YW, UK. E-mail: r.mikhaylovskiy@lancaster.ac.uk

† Electronic supplementary information (ESI) available. See **https://doi.org/10.1039/d2fd00035k**

In most cases optical excitation or THz fields trigger only a linear response of the magnetic order, *e.g.* the spin oscillations at the eigen frequencies of antiferromagnetic resonances.[4,8,9] More interesting from both fundamental and applied points of view is the possibility to trigger spin reorientation,[10] inertial switching[11] and photoinduced phase transition from antiferromagnetic to ferromagnetic states.[12,13] However, for the optical pulses this photoinduced spin-reorientation is thermal in origin and therefore inherently slow.[14] Thermal effects can also be driven by intense THz pulses manifesting as a slight shift of resonance frequency in $TmFeO_3$, thulium orthoferrite.[15] At the same time intense THz pulses can bring spins into a switching regime non-thermally. For instance all coherent spin switching was driven by a THz pulse concentrated and enhanced with a metallic antenna at the transition temperature of spin-reorientation in $TmFeO_3$.[16]

In contrast to this experimental success, the spatial inhomogeneity of the spin dynamics after excitation has been largely unexplored because only an integral magnetic moment along thickness is detected with magneto-optical effects typically used in ultrafast experiments. However, in the experiments with antennas to intensify THz amplitude[15–17] the THz field was distributed non-homogeneously and the spin dynamics is expected to propagate into the sample. Indeed, a very recent experiment revealed that strongly localised optical excitation drives propagating spin waves in an antiferromagnetic $DyFeO_3$,[18] although in a linear regime. It is an open question, however, what kind of propagating spin dynamics one can excite in the nonlinear regime with a strongly localised excitation?

Thus, our research motivation is to reveal temporal and spatial characteristics of the spin dynamics in the nonlinear regime. To this end, we construct the model to solve a partial differential equation which describes spin propagation in antiferromagnets, such as rare-earth orthoferrites. Then, we numerically calculate the spin dynamics triggered by a realistic THz pulse and vary parameters to understand the effect on nonlinearity.

Theoretical formalism

We theoretically explore spin-wave propagation in a nonlinear regime, driven by the intense terahertz pulse. In contrast to previous research, we take into account the spatial inhomogeneity of the exciting pulse and consequent propagation of the spin deflection in space. We use the Lagrangian equation of spin dynamics that yields both time evolution and spatial distribution of the magnetization as the solution.[19] For an antiferromagnet this equation has the form of a sine-Gordon equation. For the indicative case of orthoferrites, the equation of motion is given by:[16]

$$\begin{aligned}&\frac{\partial^2\phi}{\partial t^2}+\alpha\omega_{\mathrm{e}}\frac{\partial\phi}{\partial t}-C_{\mathrm{m}}^2\frac{\partial^2\phi}{\partial y^2}+\omega_{\mathrm{e}}\omega_{\mathrm{a}}\ \sin\phi\cos\phi\big(\eta(T)-\cos^2\phi\big)\\&=\xi E_{\mathrm{THz}}^2\ \sin\phi\cos\phi+\gamma\omega_{\mathrm{d}}H_{\mathrm{ext}}^{x}\ \sin\phi+\gamma\omega_{\mathrm{d}}H_{\mathrm{ext}}^{z}\ \cos\phi+\gamma\frac{\partial H_{\mathrm{ext}}^{y}}{\partial t}\end{aligned}\tag{1}$$

where α is the damping factor, C_{m} is the propagation speed limit of the spin wave, ξ is a coefficient characterising coupling between THz electric field and the spins. The function $\phi(t,y)$ represents the angle of the antiferromagnetic vector **G** in the *ac*-plane, and $\phi = 0$ if **G** is aligned along the *z*-axis; $\omega_{\mathrm{e}} = \gamma H_{\mathrm{e}}$, $\omega_{\mathrm{d}} = \gamma H_{\mathrm{d}}$, and $\omega_{\mathrm{a}} =$

$\gamma K_2/M_{Fe}$ are parameters defined for convenience, where K_2 is the constant for the fourth-order magnetocrystalline anisotropy and M_{Fe} is the magnetization of the iron sublattice. The effective magnetic fields H_d and H_e are attributed to the Dzyaloshinskii–Moriya and the exchange interactions, respectively. The constant γ is the gyromagnetic ratio. The Cartesian *xyz*-system is chosen to coincide with the crystallographic directions *a*, *b*, *c*.

Rare earth orthoferrites exhibit spin-reorientations, so the orientation of the antiferromagnetic vector flips or rotates across a specific temperature point or interval. For instance, part of orthoferrites, such as $TmFeO_3$, $ErFeO_3$ and $SmFeO_3$, have transitions from Γ_2 to Γ_4 phases as temperature increases.[8] The magnetization pointed along the *a*-axis in the Γ_2 phase moves continuously by 90 degrees to the *c*-axis in the Γ_4 phase. We focus on the intermediate Γ_{24} phase with the antiferromagnetic vector in the *ac*-plane, in which considerably large nonlinearity was reported.[20] At that phase, four equilibrium states, given by local minima of the potential energy, are placed in the *ac*-plane in the case of the zero bias field (Fig. 1b). The function $\eta(T)$ in eqn (1) defines the equilibrium orientations and reads

$$\eta(T) = -\frac{K_1}{K_2} = \frac{T_u - T}{T_u - T_l} \tag{2}$$

where the critical temperatures separating Γ_2 and Γ_{24} phases and Γ_4 and Γ_{24} phases are expressed as T_l and T_u, respectively. K_2 is the second-order magnetocrystalline anisotropy constant. The stable angle in Γ_{24} is given by $\cos^2\phi_0 = \eta(T)$.

We consider two processes of excitation *via* the electric field and magnetic field of the THz pulse separately. The first term of the right-hand side of eqn (1) represents the modulation of magnetocrystalline anisotropy by THz electric field. The high-intensity electric field E_{THz} distorts the anisotropy mediated by the orbital states of the rare-earth ions and causes the spin excitation indirectly. Other three terms

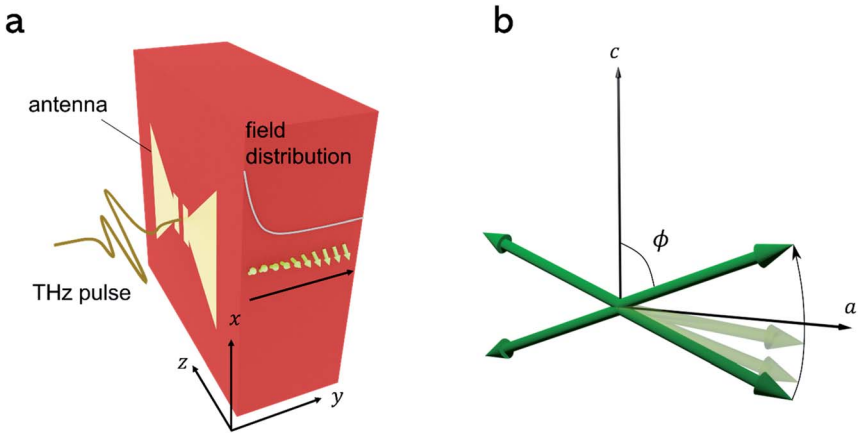

Fig. 1 Model structure for simulation. (a) The THz field is enhanced with metallic antenna fabricated on top of the orthoferrite crystal $TmFeO_3$. The incident pulse travels in the sample from the antenna side. Exponentially localised evanescent field induces spin switching and generates spin waves. (b) There are four stable positions for antiferromagnetic vector **G** in the Γ_{24} phase, especially four-fold symmetric placement in the midpoint between T_l and T_u. Through switching by external stimulation, the **G** jumps to another stable state in the *ac*-plane.

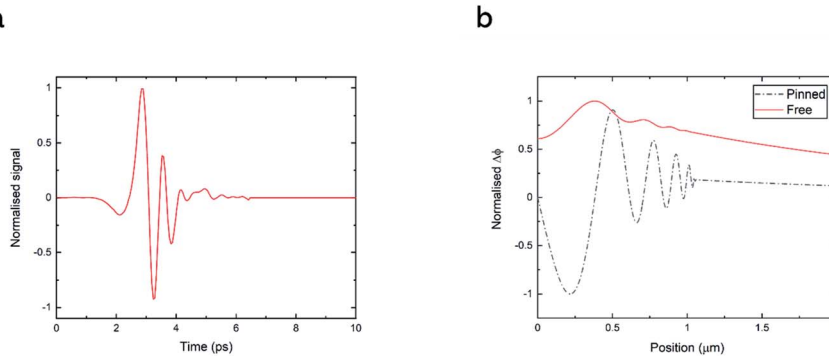

Fig. 2 (a) The THz wave form $s(t)$ used in the calculation was extracted from the real experiment. (b) The calculated snapshot of the spin deflection in the linear regime of excitation (moderate THz field strength). Two cases for different boundary conditions, Dirichlet (red solid) and Neumann (black dash-dot), are shown. The spin wave was generated from the left side where the THz field was localised by antenna enhancement.

describe Zeeman coupling, which is a direct interaction between the external magnetic field $\mathbf{H}_{ext}$ and the net magnetization. Regarding the magnetic field, we assume two origins for $\mathbf{H}_{ext}$ in this paper: the static bias field $\mathbf{H}_{bias}$ is independent of time, which alters the potential energy steadily. As a result, the symmetry in the *ac*-plane is broken; conversely, the dynamic magnetic field $\mathbf{H}_{THz}$ is caused by the pump terahertz pulse. Since the torques exerted by $\mathbf{H}_{THz}$ and $\mathbf{E}_{THz}$ are additive, we compare their effects by solving the equation while only one of these terms is present.

The shape of the terahertz pulse with amplitudes, $\mathbf{H}_{amp}$ and $\mathbf{E}_{amp}$, was taken from our measured data for the THz fields generated by tilted-pulse-front excitation and detected by electro-optical sampling.[6] The manual zero filling to the latter data was implemented to generate the longer time scale (normalised data $s(t)$ shown in Fig. 2). Furthermore, we postulated that the electric field and the magnetic field had exponential distribution with homogeneous offset in the substrate to describe the distribution of the near field in the vicinity of the antenna. The antenna fabricated on the surface enhances the terahertz signal and localizes the intensity at the neighbourhood of the antenna.[3] The distribution function is formulated as:

$$\mathbf{H}_{THz}(t,y) = \left[A\exp\left(-\frac{y}{d}\right)+1\right]\mathbf{H}_{amp}s(t), \tag{3}$$

where A is the gain of antenna and d is the spatial decay. The electric field was formed in a similar fashion:

$$\mathbf{E}_{THz}(t,y) = \left[A\exp\left(-\frac{y}{d}\right)+1\right]\mathbf{E}_{amp}s(t) \tag{4}$$

Results and discussion

Numerical modelling

We adopted a solving method called the Finite Difference Method to analyse the equation numerically. The boundary condition was mainly designated as the

Neumann (free boundary) condition, given by $\partial\phi/\partial y(y = 0) = 0$, to consider the switching phenomena. We applied all parameters for compound $TmFeO_3$, featured in recent experiments on THz spin control.[16,20] The effective fields of exchange interactions were taken from,[21] $H_d = 2 \times 10^5$ Oe and $H_e = 2 \times 10^7$ Oe. The set of transition temperatures of this material is known as approximately $T_u =$ 90 K and $T_l = 80$ K. The value $\omega_a = 2.1$ rad ns^{-1}, $\xi = 2.3 \times 10^{18}$ erg^{-1} cm^3 s^{-1} and $\alpha = 1.4 \times 10^{-4}$ was experimentally determined from the data of the quasi-ferromagnetic resonance frequency at $T = 83$ K.[3] Although those two parameters depend on frequency in a strict sense, we regarded them as constants to simplify the calculation. Besides, $C_m = 2 \times 10^6$ cm s^{-1} was used.[5]

In our calculations, the temperature was fixed at the midpoint within the spin reorientation temperature interval, namely $T = 85$ K. One of the equilibrium angles ϕ_0 in the case of the no bias field was accurately set to 45° and the others are located in the fourth-fold symmetric positions. However, the bias field slightly shifts the stationary point of the potential. This means that initial values $\phi(t = 0)$ close to $\phi = 45$ deg should be compensated adequately to remove the excitation by the bias field. After recalculation of the potential to know the new local minima with bias magnetic field, we applied initial conditions, $\phi(t = 0) = \phi_0$ and $\partial\phi/\partial t(t = 0) = 0$ and they are spatially uniform. For parameters for the field distribution, we used $A = 8$ and $d = 4$ μm, which were the values used to model the antenna response in the previous experiment.[15]

Results

At first, we calculated the spin dynamics in a linear regime with a small THz amplitude, to clarify the linear background to the nonlinearity. For the Neumann condition, the THz field $H_{THz} = 45$ kOe and the bias field $H_{bias} = 2$ kOe along the x-axis were applied. In addition, we took the Dirichlet (pinned boundary) condition, expressed as $\phi(y = 0) = 0$, with different amplitude $H_{THz} = 900$ Oe. The pinned condition can be accepted easily for the weak excitation regime, while the pinning on edges should be an unrealistic condition for strong driving and subsequent nonlinear switching phenomena. The result for both cases is illustrated in Fig. 2b. The uniform spin precession, zero-wavenumber spin wave shaped by the antenna was dominant, especially in the Neumann case. Also, the spin wave whose wavenumber was finite, not zero, propagated in spite of the much smaller amplitude than the uniform mode. These results were comparable to a previous simulation on linear propagation excited by an optical pump.[17]

Next, increasing the intensity of THz field, we stepped into the nonlinear regime. The enhanced magnetic field, $H_{THz} = 54$ kOe, induced nonlinear dynamics, involving flipping of the antiferromagnetic vector into another equilibrium orientation (Fig. 3a, see also ESI Movie 1†). This creates a non-stationary domain wall separating the regions with metastable spin orientations. The external bias $H_{bias} = 2$ kOe along the x-axis eliminated the two local minima around $\phi = \pm 135°$ (Fig. 3b). In the first part of the process in about ten picoseconds, the spin around the antenna moves to the other equilibrium position. This phenomenon is caused by inertia motion following the main peak of the THz pulse (at $t < 3$ ps in Fig. 2a). On the other hand, the angle of spins at a distant position from the antenna return to the initial position as a result of damping. This localised reversal forms a domain wall between the different spin

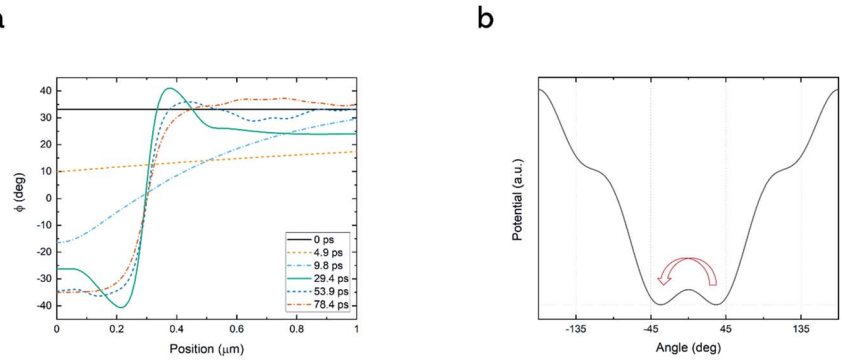

Fig. 3 (a) Snapshots of the spin deflection angle in the strongly nonlinear regime, when the bias magnetic field is applied along the x-axis. After forming the domain wall between the initial and the switched orientations, the various modes of the spin wave are emitted from the wall. (b) The potential landscape set by the bias field with the two stable states. The THz excitation enabled the spin around the antenna to flip to the alternative stable state.

orientations around $y = 0.3$ μm, and the position of the wall after the THz pulse duration is fixed all the time. The position of the domain wall is determined by the parameter d in eqn (3), the penetration depth of the THz field for the chosen wave form and spatial distribution. This position corresponds to the threshold THz amplitude, required to bring the magnetic order parameter over the potential barrier separating two equilibrium orientations (see Fig. 3b). At the same time the sudden appearance of this discontinuity generates spin waves with finite wavenumbers propagating into both positive and negative directions from the domain wall. The spin wave emission mechanisms resemble the linear regime mentioned before (Fig. 2b). The domain wall plays the role of the pinned boundary.

The different orientation of the bias field along the z-axis provide completely different results, accompanied with movement of the domain wall (Fig. 4a, ESI Movie 2†). The comparably weak bias $H_{\mathrm{bias}} = 500$ Oe along the z-axis reduced the barrier to facilitate the switching by the THz pulse with the amplitude, $H_{\mathrm{THz}} = 54$ kOe. The long-distance propagation of the wall follows from the different potential landscape (Fig. 4b). The bias modulated the symmetric potential to non-symmetric one at about $\phi = 0$ and pushed up the initial position ϕ_0 to the metastable state. The spin on this local minimum state fell down to the lower global minimum around $\phi = -45°$. This is the origin of the domain movement. Moreover, the larger amplitude of bias field, for example $H_{\mathrm{bias}} = 1$ kOe, caused the other domain wall between $\phi = -45°$ and $\phi = -135°$, which stayed at the same position (see ESI Movie 3†). The boundary was essentially the same as the result shown in Fig. 3a from the standpoint of the equal potential levels.

To compare dynamics induced by the electric field to one by the magnetic field, we applied $E_{\mathrm{THz}} = 9$ MV cm^{-1} to eqn (1) and neglected terms for the Zeeman effect. We calculated only one case with $H_{\mathrm{bias}} = 2$ kOe along the x-axis. The obtained result was quite similar (ESI Movie 4†) to the one shown in Fig. 3a because the action of E_{THz} can be seen as an effective magnetic field pulse.

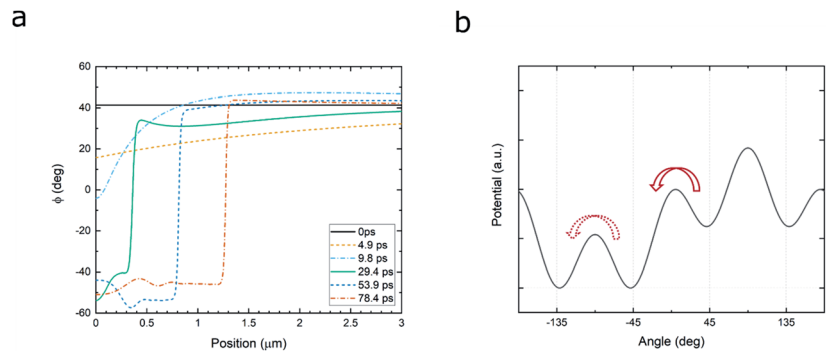

Fig. 4 (a) Snapshots of the spin deflection angle in the strongly nonlinear regime, when the bias magnetic field is applied along the z-axis and the spins are initially aligned in a metastable state. In contrast to the situation shown in Fig. 3, here the domain wall is moving away from the sample boundary. (b) The potential landscape with the bias oriented z-axis show that the main excitation occurred as a result of falling through the slope between $-45°$ and $45°$.

Conclusions

In summary, we developed the model for nonlinear and non-local spin dynamics relevant to the recent experiments with THz pump pulses concentrated by the metallic antennas fabricated on top of the antiferromagnetic sample. We predict the formation of the non-stationary and at certain conditions a moving boundary, separating stable orientations of the antiferromagnetic vector. The resulting moving discontinuity can emit spin waves. The propagation of waves through the moving boundary opens a new vistas for the non-stationary effects such as modulation of the spin wave frequencies reminiscent of propagation of the electro-magnetic waves across the relativistic boundary. We believe our theoretical results will inform and inspire future experimental work in the burgeoning field of antiferromagnetic magnonics.

Author contributions

Y. S. has performed the mathematical derivation and numerical calculations and analysis under the guidance of R. V. M., who formulated the project and supervised it.

Conflicts of interest

There are no conflicts to declare.

Acknowledgements

This work was funded by the European Research Council ERC grant agreement no. 852050 (MAGSHAKE).

References

1 T. Jungwirth, X. Marti, P. Wadley and J. Wunderlich, *Nat. Nanotechnol.*, 2016, **11**, 231–241.

2 P. Němec, M. Fiebig, T. Kampfrath and A. V. Kimel, *Nat. Phys.*, 2018, **14**, 229–241.
3 V. V. Eremenko, N. F. Kharchenko, Y. G. Litvinenko and V. M. Naumenko, *Magneto-Optics and Spectroscopy of Antiferromagnets*, Springer, 1992.
4 A. V. Kimel, A. Kirilyuk, P. A. Usachev, R. V. Pisarev, A. M. Balbashov and T. Rasing, *Nature*, 2005, **435**, 655–657.
5 J. Hebling, G. Almasi, I. Kozma and J. Kuhl, *Opt. Express*, 2002, **10**, 1161.
6 T. Kampfrath, A. Sell, G. Klatt, A. Pashkin, S. Mährlein, T. Dekorsy, M. Wolf, M. Fiebig, A. Leitenstorfer and R. Huber, *Nat. Photonics*, 2011, **5**, 31–34.
7 T. Suemoto, K. Nakamura, T. Kurihara and H. Watanabe, *Appl. Phys. Lett.*, 2015, **107**, 042404.
8 A. M. Kalashnikova, A. V. Kimel, R. V. Pisarev, V. N. Gridnev, P. A. Usachev, A. Kirilyuk and T. Rasing, *Phys. Rev. B: Condens. Matter Mater. Phys.*, 2008, **78**, 104301.
9 T. Satoh, S.-J. Cho, R. Iida, T. Shimura, K. Kuroda, H. Ueda, Y. Ueda, B. A. Ivanov, F. Nori and M. Fiebig, *Phys. Rev. Lett.*, 2010, **105**, 077402.
10 A. V. Kimel, A. Kirilyuk, A. Tsvetkov, R. V. Pisarev and T. Rasing, *Nature*, 2004, **429**, 850–853.
11 A. V. Kimel, B. A. Ivanov, R. V. Pisarev, P. A. Usachev, A. Kirilyuk and T. Rasing, *Nat. Phys.*, 2009, **5**, 727–731.
12 T. Li, A. Patz, L. Mouchliadis, *et al.*, Femtosecond switching of magnetism via strongly correlated spin–charge quantum excitations, *Nature*, 2013, **496**, 69–73.
13 D. Afanasiev, B. A. Ivanov, A. Kirilyuk, T. Rasing, R. V. Pisarev and A. V. Kimel, *Phys. Rev. Lett.*, 2016, **116**, 097401.
14 J. A. de Jong, I. Razdolski, A. M. Kalashnikova, R. V. Pisarev, A. M. Balbashov, A. Kirilyuk, T. Rasing and A. V. Kimel, *Phys. Rev. Lett.*, 2012, **108**, 157601.
15 Y. Mukai, H. Hirori, T. Yamamoto, H. Kageyama and K. Tanaka, *New J. Phys.*, 2016, **18**, 013045.
16 S. Schlauderer, C. Lange, S. Baierl, T. Ebnet, C. P. Schmid, D. C. Valovcin, A. K. Zvezdin, A. V. Kimel, R. V. Mikhaylovskiy and R. Huber, *Nature*, 2019, **569**, 383–387.
17 T. Kurihara, H. Watanabe, M. Nakajima, S. Karube, K. Oto, Y. Otani and T. Suemoto, *Phys. Rev. Lett.*, 2018, **120**, 107202.
18 J. R. Hortensius, D. Afanasiev, M. Matthiesen, R. Leenders, R. Citro, A. V. Kimel, R. V. Mikhaylovskiy, B. A. Ivanov and A. D. Caviglia, *Nat. Phys.*, 2021, **17**, 1001–1006.
19 A. K. Zvezdin, *Pis'ma Zh. Eksp. Teor. Fiz.*, 1979, **10**, 605.
20 S. Baierl, M. Hohenleutner, T. Kampfrath, *et al.*, *Nat. Photonics*, 2016, **10**, 715–718.
21 A. M. Balbashov, G. V. Kozlov, A. A. Mukhin and A. S. Prokhorov, in *High Frequency Processes in Magnetic Materials*, World Scientific, 1995, pp. 56–98.